

Electron and Hole Drift Mobilities in Vitreous Selenium

H. P. GRUNWALD

Department of Physics, Union College, Schenectady, New York

AND

R. M. BLAKNEY*

Institute of Optics, University of Rochester, Rochester, New York

(Received 14 August 1967)

The drift mobilities for electrons and holes in vitreous Se were measured as a function of temperature and as a function of the applied electric field. The drift mobilities exhibited a temperature dependence not previously observed. The electron drift mobility exhibited an exponential temperature dependence up to the glass transition temperature ($T_g=305^\circ\text{K}$). At this point, a sharp break from the exponential temperature dependence was observed. Below 305°K , the electron drift mobility exhibited an exponential temperature dependence which is characteristic of a trap-limited drift process. In this temperature range, the computed mobility-controlling electron trap densities and the measured activation energies depended on the temperature of the substrate at which the selenium films were prepared. It is shown that as the substrate temperature is increased, the activation energy for the mobility increases, and the density of the traps which control the mobility decreases. The hole drift mobility exhibited an exponential temperature dependence at low temperatures, but a gradual deviation from the exponential temperature dependence at a temperature of about 260°K was observed. This indicates that the microscopic hole mobility μ_{0p} has a low value. The microscopic hole mobility, evaluated at 293°K , yielded an average value of $\mu_{0p}=0.34 \pm 0.05 \text{ cm}^2\text{V}^{-1} \text{ sec}^{-1}$. In the low-temperature range the hole trap densities and the activation energies were computed. These quantities revealed the same dependence on the substrate preparation temperature as the corresponding quantities for electron transport. It is postulated that the mobility-controlling traps are caused by the disorder in the amorphous selenium. The electron and hole drift-mobility values at room temperature agreed with previous measurements.

I. INTRODUCTION

CARRIER drift mobilities in evaporated films of elemental amorphous selenium have been measured by Spear¹ (1957, 1960) and by Hartke² (1962). Both authors found that the electron and hole drift mobilities depended on the temperature as $\exp(-E/kT)$, where k is Boltzmann's constant, and E is the energy depth of the mobility-controlling traps from the band edge. Spear measured activation energies of 0.25 and 0.15 eV, while Hartke measured activation energies of 0.285 and 0.14 eV for electron and hole mobilities, respectively. These measurements indicated that the electron mobility is controlled by trapping states about 0.25 eV below the conduction band, and the holes by trapping states 0.14 eV above the valence band. No deviations from the simple exponential law were reported by Spear, while Hartke reported anomalous decreases in drift mobilities at about 243 and near 261°K for holes and electrons, respectively. It was proposed that these anomalies are due to structural changes in the films due, possibly, to the difference in the thermal expansion coefficient between the selenium and the substrate. Some correlation was thought to exist between the observed temperature of the anomalies and the temperature at which physical damage to the film occurred.

In this paper the drift mobilities are reexamined. It will be shown that the activation energies depend on the sample preparation and that the electron and hole mobilities obey the simple exponential law only at low temperatures.

II. EXPERIMENTAL PROCEDURE

Unsupported amorphous selenium films of about 60μ thickness and of 1 cm diam were prepared by vacuum evaporation onto aluminum-foil substrates, whose temperatures were monitored and held constant to within $\pm 2^\circ\text{C}$. Substrate temperatures ranged from 25 to 60°C , evaporation times were of about 30–40 min duration during which the crucible temperature was held at 320°C . The experimental arrangement and the sample mounting have previously been described in detail and are summarized below.³ The selenium sample was separated from the aluminum foil and was placed between two thin ($\approx 1 \mu$ thick) blocking layers of Pyrex. The resulting sandwich was clamped between two parallel electrodes one of which was transparent. A short pulse (60-nsec duration at $1/e$) of strongly absorbed light was incident on the transparent electrode. The thin sheet of charge so generated at the surface drifted under an applied electric field through the film, the type of carrier observed depended on the direction of the field. The resulting voltage pulse was amplified, electronically differentiated, and directly photographed from the oscilloscope screen. Figure 1

* Present address: E. H. Plessett Associates, Inc., Santa Monica, Calif.

¹ W. E. Spear, Proc. Phys. Soc. (London) **B70**, 669 (1957); **B76**, 826 (1960).

² J. L. Hartke, Phys. Rev. **125**, 1177 (1962).

³ R. M. Blakney and H. P. Grunwald, Phys. Rev. **159**, 664 (1967).

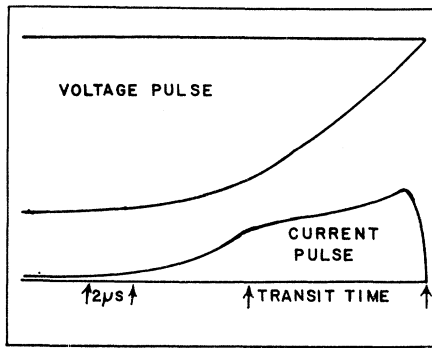


FIG. 1. Observed oscilloscope trace showing the voltage pulse (upper trace) and the transient current (lower trace). The rapid drop in the current indicates the transit time of the injected electrons in an applied field of 1.57×10^5 V cm $^{-1}$ at 285°K. The electrode area was approximately 0.4 cm 2 and the film thickness was 55 μ .

shows an observed oscilloscope trace displaying both the voltage pulse (upper trace) and the current (lower trace) as a function of time. These traces are for electrons drifting in a 54.6- μ Se layer in an applied field of 1.57×10^5 V cm $^{-1}$ at a temperature of 285°K. The rapid drop in the current transient indicates the transit time of the injected electrons. Note that the rapid drop in the current clearly indicates the transit time of the injected electrons, while this point is not evident in the voltage trace.

In this experiment the transit time T_r was determined from the time of the sharp break in the current trace. However, at high fields, the transit time approached the time constant of the differentiating circuit (1 μ sec) and a determination of T_r from the current trace was not possible. Under these conditions, however, the voltage trace exhibited a well-defined break at the transit time. Therefore, for $T_r \geq 1.4$ μ sec, the time of rapid drop in the current trace was used as a measure of the transit time, while for $T_r \leq 1.4$ μ sec the time of sharp levelling off of the voltage pulse was taken as a measure of the transit time. The latter method was used by Spear¹ and by Hartke² over the whole temperature interval as a definition of transit time. In this experiment it was necessary to use this technique for holes above 20°C.

The validity of the technique depends on the trapping kinetics of the charge carrier. In the simplest case, when only deep traps are present, the Hecht equation gives a simple validity criterion,

$$Q(t) = eN_0\mu_d E(T_t/L)[1 - \exp(-t/T_t)]. \quad (1)$$

Here $Q(t)$ is the charge induced on the sample electrodes, N_0 are the number of charge carriers injected, μ_d is the drift mobility, $E = V/L$ is the applied electric field, and T_t is the trapping time. Therefore at time $t = T_r = L/\mu_d E$ a sharp levelling off of the voltage pulse is observed if the Schubweg (W) satisfies the condition $W = \mu_d E T_t \gg L$, while for the condition $W < L$ the rise time of the voltage pulse is determined by trapping. It is

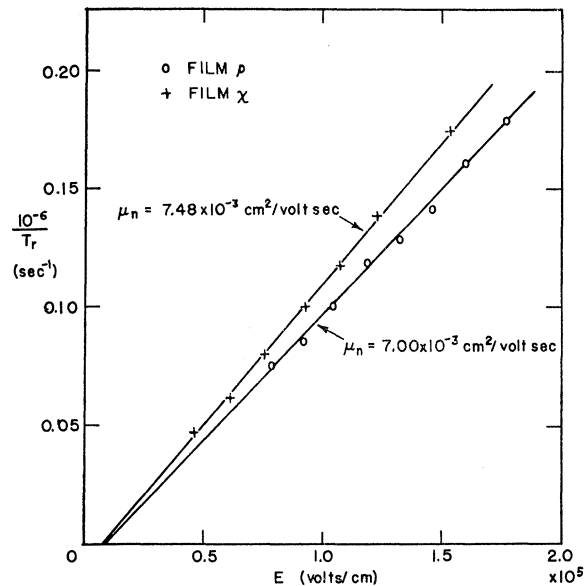


FIG. 2. Inverse transit time of electrons at 302°K versus the applied electric field for films ρ (66.0 μ thick) and χ (62.2 μ thick). The electron drift mobility μ_n was calculated from the slope of these lines.

apparent that the above criterion applied to the current transient is observable as a sharp break (Fig. 1), in the current trace if the condition $W > L$ is applicable. If instead the condition $W < L$ applies, this sharp break disappears. The lowest temperature at which transit times could be measured was then determined by the above condition.

III. EXPERIMENTAL RESULTS

The transit time T_r as described above was measured for a number of selenium films as a function of temperature from which the drift mobility was obtained from $\mu_d = L^2/(T_r V)$. The results of these measurements are summarized below:

(a) In Fig. 2, the inverse transit time for electrons is plotted as a function of the applied electric field at a temperature of 302°K. The electron drift mobility μ_n computed from the slope of these linear plots is shown in the figure. The drift mobilities at 302°K lie between 6.6×10^{-3} and 8.0×10^{-3} cm 2 V $^{-1}$ sec $^{-1}$, for all films, and no consistent variation with substrate temperature was observed. The maximum error in the determination of the electron drift mobility is probably due to the thickness measurement of the sample. The magnitude of the electron drift mobility as determined by us is in excellent agreement with the measurements by Spear and by Hartke.

(b) The results of the electron drift-mobility measurements over the temperature range 246–320°K are tabulated in Table I. In Fig. 3, we have plotted the logarithm of μ_n against the inverse temperature, for

TABLE I. Amorphous selenium drift^a parameters.

Film	Substrate temp. (°C)	N_c/N_{in} at 293°K	μ_n (cm ² /V sec) at $T=293^\circ\text{K}$	E_n (eV)	N_v/N_{ip} at 293°K	μ_p (cm ² /V sec) at $T=293^\circ\text{K}$	μ_{op} (cm ² /V sec) at $T=293^\circ\text{K}$	E_p (eV)
ρ	58	7.35×10^3	4.5×10^{-3}	0.332
σ	58	8.91×10^3	5.4×10^{-3}	0.323	8.8×10^3	0.12	0.32	0.247
τ	48	3.4×10^3	5.7×10^{-3}	0.307	5.9×10^3	0.11	0.30	0.235
χ	38	2.06×10^3	5.8×10^{-3}	0.294	1.2×10^3	0.12	0.36	0.200
ψ	25	1.56×10^3	4.6×10^{-3}	0.287	1.5×10^3	0.11	0.36	0.210
Spear	20	3.12×10^2	5.2×10^{-3}	0.25	...	0.135	...	0.14

^a See Ref. 6.

two of the samples. It can be seen that an exponential law is followed for temperatures below 305°K.

(c) It will be observed in Fig. 3 that the slope of $\ln \mu_n$ as a function of $1/T$ undergoes an abrupt change at 305°K ($10^3/T=3.28$) and is constant in the temperature range 305–320°K. (Measurements above 320°K were not taken because a rapid conversion from vitreous to hexagonal selenium occurs above this temperature). The temperature at which the abrupt change in the slope occurred was repeatable from sample to sample and the data for each sample was reproducible in traversing the temperature range in both directions.

(d) In Fig. 4, the measured activation energy for electron transport is plotted as a function of the substrate temperature. It is seen that the activation energy depends linearly on the substrate temperature over the range investigated.

(e) In Fig. 5, the inverse transit time for holes for film σ is plotted as a function of the applied electric

field at a temperature of 301°K. The hole drift-mobility value of $\mu_p=0.14 \text{ cm}^2 \text{ V}^{-1} \text{ sec}^{-1}$ is also in excellent agreement with the measurements of Spear and Hartke. It is to be noted here also, that the room-temperature mobility for all the films is the same, to within the experimental error.

(f) The results of the hole drift-mobility measurements over the temperature range 200–320°K are also tabulated in Table I. In Fig. 6, we have plotted the logarithm of μ_p against the inverse temperature for one of the samples. It can be seen that the mobility exhibits an exponential dependence below about 260°K. Above 260°K the hole mobility deviates gradually from the exponential law.

(g) In Fig. 4, the measured activation energy for hole transport is plotted as a function of the substrate temperature. It is seen that the activation energy for hole transport also depends linearly on the substrate temperature over the range investigated.

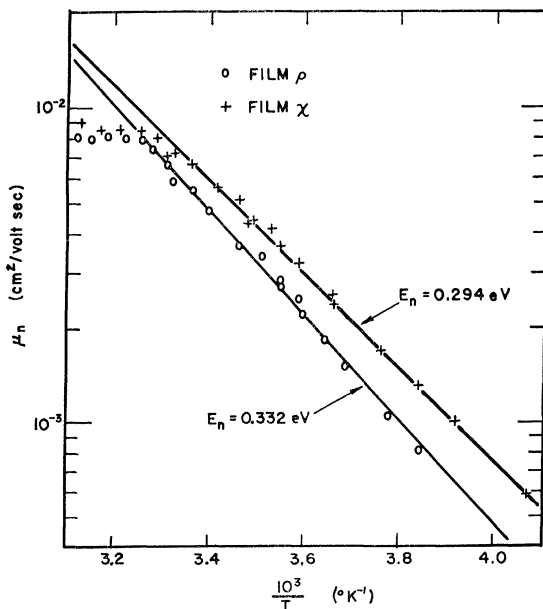


FIG. 3. Temperature dependence of the electron drift mobility for two amorphous selenium films. The abrupt change in slope at 305°K is clearly indicated. The applied electric fields were 7.72×10^4 and $1.23 \times 10^5 \text{ V cm}^{-1}$ for films ρ and χ , respectively.

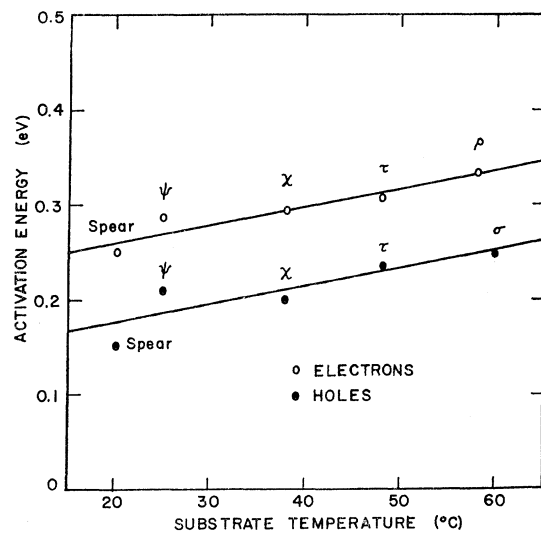


FIG. 4. The activation energy for electron and hole transport versus the substrate temperature used in the preparation of the samples. The activation energies measured by Spear at an estimated substrate temperature are also plotted. The Greek letters identify the samples.

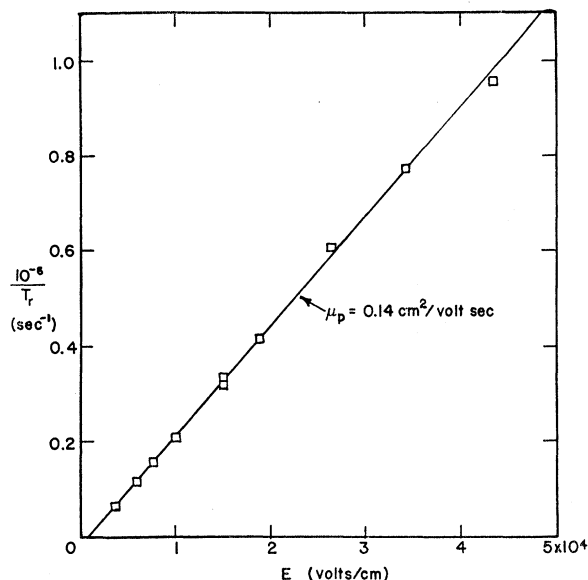


FIG. 5. Inverse transit time of holes at 301°K versus the applied electric field for film σ (61.0 μ thick). A hole drift mobility of 0.14 $\text{cm}^2 \text{V}^{-1} \text{sec}^{-1}$ was computed from the slope.

IV. DISCUSSION

The observed drift mobilities can be explained in terms of a trap-controlled mobility. The physical picture is that the charge carrier while moving through the film is trapped then liberated into the mobile state where it is occasionally scattered by phonons until re-trapping occurs. For the case of electrons the appropriate expression relating the electron drift mobility μ_n and the microscopic mobility μ_{0n} is

$$\mu_n = \mu_{0n} \tau_{0n} / (\tau_{0n} + \tau_{dn}), \quad (2)$$

where τ_{0n} is the mean free time of an electron in the conduction band and τ_{dn} is the time of dwell of an electron in a trap. For the case of a discrete trapping level of density N_{tn} at energy depth E_n below the conduction band [Eq. (2)] leads to the expression

$$\mu_n = \mu_{0n} [1 + (N_{tn}/N_c) \exp E_n/kT]^{-1}, \quad (3)$$

where N_c is the effective density of state s at the bottom of the conduction band. The corresponding equation for the hole drift mobility μ_p with the appropriate definition of symbols is apparent. In the temperature range when $\tau_{dp} > \tau_{0p}$ [Eq. (3)] can be approximated by

$$\mu_p = \mu_{0p} (N_c/N_{tp}) \exp(-E_n/kT). \quad (4)$$

From this equation the ratio N_c/N_{tp} can be evaluated if μ_{0p} is known. We assumed that the microscopic mobility μ_{0p} is equal to the Hall mobility and evaluated N_c/N_{tp} using $\mu_{0p} = 0.32 \pm 0.1 \text{ cm}^2 \text{V}^{-1} \text{sec}^{-1}$ at 293°K as measured by Dresner.⁴ In Table I, these ratios are

⁴ J. Dresner, J. Phys. Chem. Solids 25, 505 (1964).

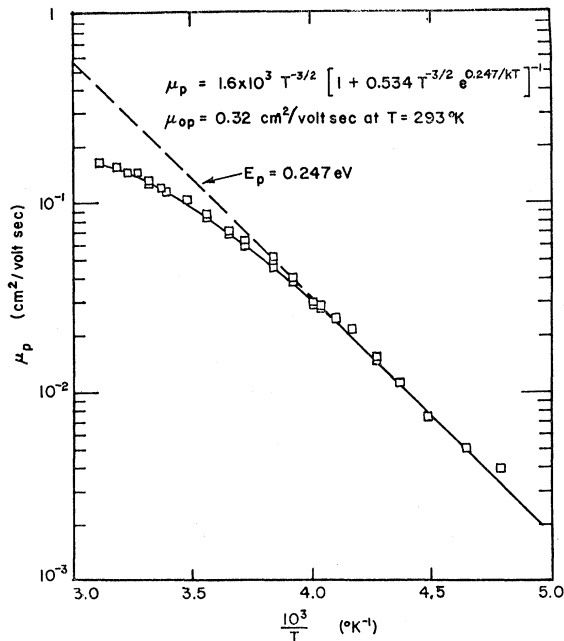


FIG. 6. Temperature dependence of the hole drift mobility for film σ . The low-temperature exponential and the deviation from this exponential above 260°K is shown. The solid line is a fit to the experimental data using the equation given in the figure.

tabulated for several samples. The result of Spear is also listed at an estimated substrate preparation temperature.

Let us assume that N_c does not vary with the substrate temperature. Then, by comparing the ratio N_c/N_{tp} and the corresponding activation energy for each film, one sees that as the substrate temperature is increased, the activation energy for the mobility increases, and the density of the traps which control the mobility decreases.

The temperature (305°K) at which the sharp deviation from the exponential law occurs, coincides with the glass transition temperature T_g of selenium and it is very probable that these two facts are related. From a consideration of the viscoelastic properties of amorphous selenium as a function of temperature, Eisenberg and Tobolsky⁵ determined T_g to be $304 \pm 0.5^\circ\text{K}$. Although the glass transition temperature is a property shared by many compounds, its physical nature is as yet not completely understood. Gibbs⁶ believes that this phenomena is a second-order transition in the sense of Ehrenfest; that is, the Gibbs function and its first derivative are continuous while the second derivative is discontinuous at the transition temperature. This implies that a change of slope occurs in such thermo-

⁵ A. Eisenberg and A. V. Tobolsky, J. Polymer Sci. 61, 483 (1962).

⁶ J. H. Gibbs, in *Modern Aspects of the Vitreous State*, edited by J. D. Mackenzie (Plenum Press, Inc., New York, 1960), Vol. I, p. 152.

dynamic quantities as the entropy versus temperature and the volume versus temperature curves. He further suggests that the transition is due to a limited number of configurations available to the system below the transition temperature and that this number greatly increases above T_g . Here the term "configuration" implies the specification of the locations, orientations and shapes of all the molecules in the system. This suggests a possible explanation for the electron drift-mobility data above the sharp break is that the density of localized states N_{tn} increases as a function of temperature reversibly due to these additional possible configurations above the glass transition temperature. This in turn suggests that the origin of the traps is closely linked with the disorder itself. We believe that below the glass transition temperature T_g the short-range order is frozen into the amorphous selenium film but that a rapid change in the short-range order occurs above T_g .

The starting point for a discussion of the hole drift mobility is Eq. (3) with the appropriate symbols for holes:

$$\mu_p = \mu_{0p} [1 + (N_{tp}/N_v) \exp(E_p/kT)]^{-1}. \quad (5)$$

In the low-temperature range, the approximation

$$\mu_p = \mu_{0p} (N_v/N_{tp}) \exp(-E_p/kT) \quad (6)$$

is again valid. In Table I the activation energies E_p computed from Eq. (6) are tabulated. The gradual deviation from the simple exponential, Eq. (6), indicates that the low-temperature approximation is not valid in the upper temperature range, so that the data must be interpreted via Eq. (5). The microscopic mobility μ_{0p} and the ratio N_v/N_{tp} can then be evaluated by fitting the experimental data with the theoretical expression. These quantities are given in Table I for several samples.

In the evaluation of these parameters, it was assumed that μ_{0p} in Eq. (5), is determined by lattice scattering and is proportional to $T^{-3/2}$ and that the effective density of states in the valence band is proportional to $T^{+3/2}$. Figure 6 shows a typical plot of the logarithm of the drift mobility against $1/T$. The solid line is a fit of Eq. (5) to the experimental data, with the parameters as given in the figure. The low-temperature

exponential is shown as a dashed line. For all films examined, an average value for the hole lattice mobility of $\mu_{0p} = 0.34 \pm 0.05 \text{ cm}^2 \text{ V}^{-1} \text{ sec}^{-1}$ at 293°K was computed. This supports the deductions by Dresner,⁴ who tried without success to detect the fast holes ($\mu_{0p} \approx 60 \text{ cm}^2 \text{ V}^{-1} \text{ sec}^{-1}$) predicted by Spear.¹ Dresner estimated that μ_{0p} cannot be greater than $3 \text{ cm}^2 \text{ V}^{-1} \text{ sec}^{-1}$ and is very likely close to $0.1 \text{ cm}^2 \text{ V}^{-1} \text{ sec}^{-1}$. Our results bear out this conclusion.

In Table I we have also tabulated the ratios N_v/N_{tp} for several samples. Let us again assume that N_v does not vary with the substrate temperature. Then here, as in the case of the electron trap densities, an increasing activation energy with increasing substrate temperature is in evidence and is associated with a decreasing trap density.

Above the glass transition temperature, no abrupt change in the behavior of the hole drift mobility was observed. In this temperature range, the second term in Eq. (5) is less than unity and a small change in the magnitude of the second term is partially masked by the magnitude of the first term. At the same time, a change in N_{tp} of about 25% would have prevented a good fit of Eq. (5) to the experimental data of Fig. 6. We thus conclude that N_{tp} changes by less than 25% above the glass transition temperature.

V. CONCLUSIONS

The evaluation of the parameters, especially the trap densities, depend to a large extent on the physical model adopted. However, within this limitation, a number of conclusions are possible:

- (1) The activation energies for electron and hole drift depend linearly on the substrate temperature.
- (2) The trap densities for electrons and holes increase as the substrate temperature decreases.
- (3) A correlation exists between the trap density and the activation energy.
- (4) At 305°K a sudden change of slope occurs in the $\ln \mu_n$ versus T^{-1} graph, probably due to a change in short-range order.
- (5) The hole microscopic mobility at 293°K is $\mu_{0p} = 0.34 \pm 0.05 \text{ cm}^2 \text{ V}^{-1} \text{ sec}^{-1}$.